

Numerical Approach Investigation of Projectile with Boattail

Haibo Lu ^{a*}, Zhihong Ye ^b and Deyou Xu ^c

Artillery Military Theory Innovation and Operation Experiment Center, Army Academy of Artillery and Air Defense, Nanjing 211132, China

^alhboo@sohu.com, ^bsubmission621@163.com, ^c13915947445@139.com

Keywords: Boattail; Projectile with base cavity; Aerodynamic drag; Flow field; Numerical simulation

Abstract. The paper focuses on the influence of boattail on the flow field and aerodynamic force of the projectile. With the same base cavity, projectiles without and with boattail (boattail angle, 2°) are simulated numerically. The flow field parameters and the aerodynamic drag coefficient of models were obtained. The numerical results show that there is one more expansion wave is formed which is caused by the boattail configuration. This expansion wave weakens the one at the bottom of the projectile and decreases the base pressure of the projectile. The aerodynamic drag is decreased too.

Introduction

The boattail is an effective configuration for projectile to decrease the aerodynamic drag, many investigations have been done in this field [1-8]. The boat tail configuration is helpful to weaken the violent expansion wave at the bottom of the projectile, the base pressure of the projectile is decreased. Nowadays, the boat tail configuration is used wildly on large and medium caliber gun.

In the paper, the influence of the boattail angle on the flow field and aerodynamic drag of the projectile with base cavity is investigated numerically. The difference of the flow field between projectile with or without boattail is compared for the further research.

Numerical Method

Governing Equations For the characteristic of the flow of the projectile, the axisymmetric Navier-Stokes equations [9] are used in the simulation. The N-S equation is given by

$$\frac{\partial U}{\partial t} + \frac{\partial E}{\partial x} + \frac{\partial F}{\partial r} + \frac{S}{r} = \frac{1}{\text{Re}} \left(\frac{\partial E_v}{\partial x} + \frac{\partial F_v}{\partial r} + \frac{H}{r} \right) \quad (1)$$

$$U = \begin{bmatrix} \rho \\ \rho u \\ \rho v \\ e \end{bmatrix}, E = \begin{bmatrix} \rho u \\ \rho u^2 + p \\ \rho uv \\ u(e+p) \end{bmatrix}, F = \begin{bmatrix} \rho v \\ \rho uv \\ \rho v^2 + p \\ v(e+p) \end{bmatrix}, S = \begin{bmatrix} \rho v \\ \rho uv \\ \rho v^2 \\ v(e+p) \end{bmatrix}, E_v = \begin{bmatrix} 0 \\ \tau_{xx} \\ \tau_{xr} \\ q_x \end{bmatrix}, F_v = \begin{bmatrix} 0 \\ \tau_{rx} \\ \tau_{rr} \\ q_r \end{bmatrix}, H = \begin{bmatrix} 0 \\ \tau_{rx} \\ \tau_{rr} \\ q_r \end{bmatrix}$$

where x is the flow direction, r is the radial, τ is the shearing stress, q is the heat flux, ρ is the density of the free stream, u is the axial velocity of the free stream, v is the radial velocity of the free stream, T is the temperature of the free stream, p is the pressure of the free stream, e is the energy per unit mass fluid ($e = \rho [C_v T + (u^2 + v^2)/2]$) of the free stream.

The $k-\varepsilon$ turbulence model [10] is used. The convective term is approximated with the Van Leer splitting method [11], and the central difference method is used for the viscous terms. The LU-SSOR scheme is used for the time integration.

Grid and Boundary Conditions As shown in Fig. 1, the grid of the projectile (with boattail angle 2°) is given.

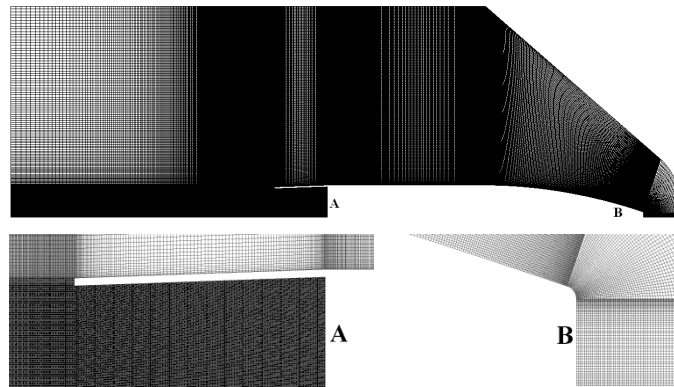


Figure 1. Grid of the simulation model (with boattail angle 2°)

The wall boundary condition is assumed to be no-slip and adiabatic. The flow conditions of the free stream are shown in Table 2.

Table 1 Boundary conditions

Free stream parameter	Unit	Value
Mach Number (Ma)	----	1.97
Pressure (p_∞)	Pa	101325
Temperature (T_∞)	K	300

Results and Discussions

Flow field The distributions of Ma contours and streamlines of the projectile with base cavity but without boattail angle is shown in Fig. 2 and Fig. 3 is the projectile with boattail angle (2°). As shown, a classical flow field is formed around the projectile. There is a detached bow shock wave in front of projectiles. At the bottom of the projectile, there is a violent expansion wave and a large recirculation region in the base cavity. The enlarged drawing of Ma contours and streamlines located in base cavity area of the flow field is shown in Fig. 4 and Fig. 5. These enlarged drawings show the difference between the projectile with or without boattail. To the projectile with boattail, there is an obviously outward expansion of the recirculation region near the bottom of the projectile. But at the same place of the projectile with boattail, the circumfluence is smooth more.

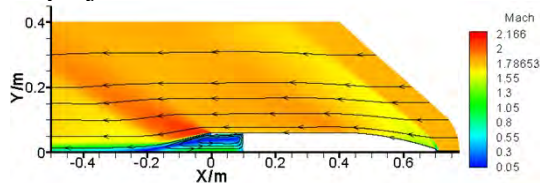


Figure 2. Ma (streamline) distribution (without boattail)

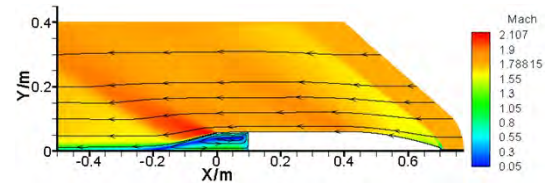


Figure 3. Ma (streamline) distribution (with boattail angle 2°)

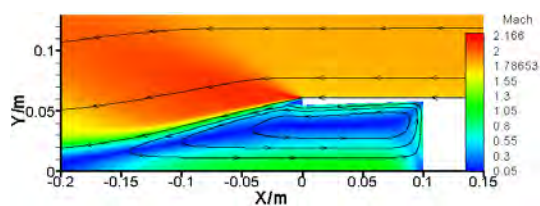


Figure 4. Local enlarged drawing of the Ma -streamline distribution (without boattail)

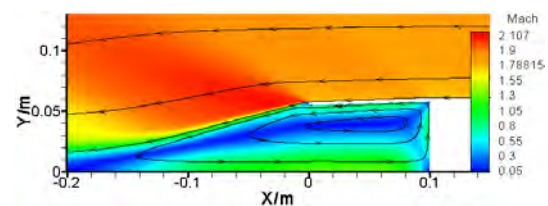


Figure 5. Local enlarged drawing of the Ma -streamline distribution (with boattail angle 2°)

In Fig. 6 and Fig. 7, the distributions of the temperature of the projectile with or without boattail are shown. A local high temperature region is formed inside the base cavity and the max temperature is located there. The distributions of the pressure of the projectile with or without boattail are given in Fig. 8 and Fig. 9. As shown in Fig. 9, there are two expansion wave formed around the projectile with boattail configuration. Before the expansion wave formed at the bottom, which the projectile without boattail configuration has too, there is another expansion because of the boattail. For the projectile with boattail, the first expansion wave weakens the second one effectively.

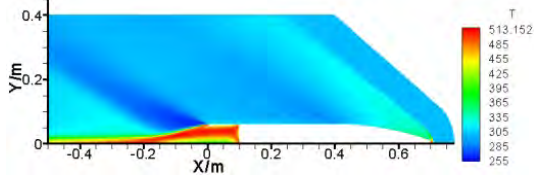


Figure 6. Temperature distribution (without boattail)

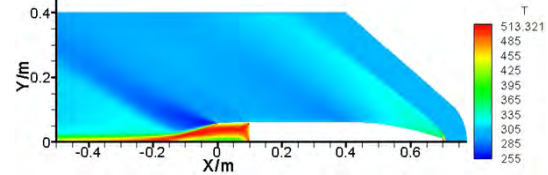


Figure 7. Temperature distribution (with boattail angle 2°)

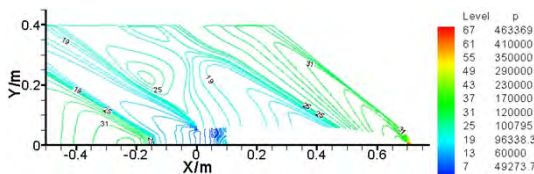


Figure 8. Pressure distribution (without boattail)

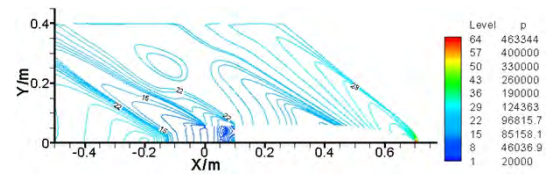


Figure 9. Pressure distribution (with boattail angle 2°)

Aerodynamic drag The drag coefficient (C_d) of the projectile is given by:

$$C_d = F_d / \left(\frac{1}{2} \rho u^2 \cdot S_{ref} \right) \quad (1)$$

where F_d is the drag force, S_{ref} is the reference area (the cross section of the projectile at cylindrical region) .

The aerodynamic drag coefficient of the projectile with boattail (2°) is 0.3018, and the coefficient of the projectile without boattail is 0.3173. For the projectile with boattail, the expansion wave, which is located at the bottom of the projectile, is weakened by the one in front of it, which is caused by the boattail configuration (Fig. 9). This is helpful to increase the base pressure of the projectile and decrease the aerodynamic drag.

Conclusion

With the same base cavity configuration, projectiles without and with boattail (boattail angle, 2°) were investigated numerically. The distribution of the flow field and the aerodynamic drag of the projectile under a supersonic flow condition were obtained. Compared with the simulation results, the aerodynamic drag is decreased by the boattail configuration is useful to increase the base pressure of the projectile.

References

- [1] Zhou Changfei, Feng Feng, Wu Xiaosong. Research on base flow field and aerodynamic characteristics of the supersonic base bleed projectile. ACTA Aerodynamica Sinica, 32(6), 783-790 (2014). (in Chinese)
- [2] Ding Zesheng, Lo Yong, Chen Shaosong, Li Jingyuan. An Investigation of the After Body Shape Effects of Nonfinned and Finned Projectiles on the Drag Reduction Characteristics of Base Bleed. Journal of Ballistics, 11(1), 80-87 (1992). (in Chinese)

- [3] Tan Junjie, Wang Fuhua, Xu Qin, Zhao Runxiang. The Experimental Investigation and analysis about the Effects of Tail Sting and Boat Tail on the Base Pressure of Projectiles at Supersonic. *Experiments and Measurements in Fluid Mechanics*, 11(4), 13-17 (1997). (in Chinese)
- [4] Ma Jie; Chen Zhihua; Zhao Qiang. Considerations of Base Shape on Aerodynamics of Supersonic Spin-Stabilized Projectile. *International Conference on Intelligent Computation Technology and Automation*, 314-317 (2015).
- [5] Kumar Amitesh, Panda H. S., Biswal T. K. etc. Flow Around a Conical Nose with Rounded Tail Projectile for Subsonic, Transonic, and Supersonic Flow Regimes : A Numerical Study. *Defence Science Journal*, 64(6),509-516 (2014).
- [6] DeSpirito James, Silton Sidra I., Weinacht Paul. Navier-Stokes Predictions of Dynamic Stability Derivatives: Evaluation of Steady-State Methods. *Journal of Spacecraft and Rockets*, 46(6),1142-1154 (2009).
- [7] Ibrahim A., Filippone A. Effect of porosity strength on drag reduction of a transonic projectile. *Journal of Aircraft*, 44(1),310-316 (2007).
- [8] Sivasubramanian J., Fasel H. F. LES and DES of high Reynolds number, supersonic base flows with control of the near wake. *Proceedings of the HPCMP Users Group Conference*, pp. 80-88 (2006).
- [9] X.S. Wu, The numerical investigation on flow field of projectile (with base bleed), *Journal of ballistics*, 4, 39-43 (1992). (in Chinese)
- [10] W.Q. Tao, *Numerical Heat Transfer*, 2nd ed. Xi' an: Xi'an Jiaotong University Press, 2001 (in Chinese)
- [11] X.D. Wang, J.J. Tan, X.H. Lin and Z.H. Tang, Research on parallel numerical simulation of N-S equations based on Van Leer+AUSM scheme, *Journal of Astronautics*, 31, 986-992 (2010). (in Chinese)